Supporting Information

Bioinspired Pomegranate-like Microflowers Confining Core-shell Binary Ni_xS_y Nanobeads for Efficient Supercapacitors Exhibiting Durable Lifespan Exceeding 100 000 circles

*Cheng Yang, Minjie Shi, Yuyu Tian, Jun Yang, Xuefeng Song, * Liping Zhao, Jing Liu, Peng Zhang, Lian Gao**

C. Yang, Y. Y. Tian, Prof. X. F. Song, Prof. L. P. Zhao, Prof. J. Liu, Prof. P. Zhang, Prof. L. Gao
State Key Laboratory for Metallic Matrix Composite Materials, School of Materials Science and Engineering, Shanghai Jiao Tong University, Shanghai 200240, P. R. China

Dr. M. J. Shi

School of Materials Science and Engineering, Jiangsu University of Science and Technology, Zhenjiang, 212003, P. R. China.

Prof. J. Yang
Shanghai Electrochemical Energy Devices Research Center, School of Chemistry and Chemical Engineering, Shanghai Jiao Tong University, Shanghai 200240, P. R. China

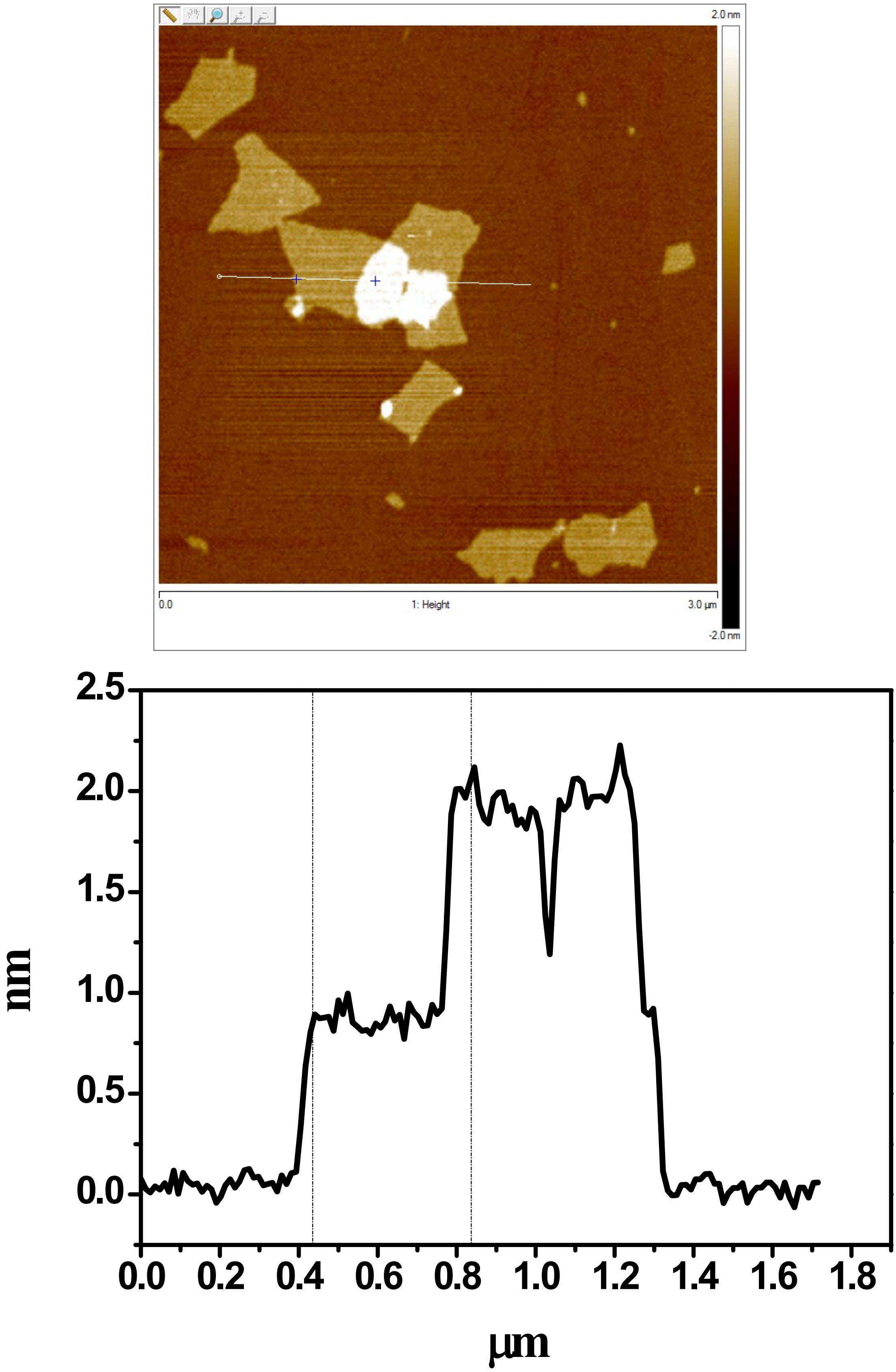

Fig. S1. The atomic force microscope (AFM) image of graphene oxide sheets. The thickness of graphene nanosheets is about 0.48 nm.

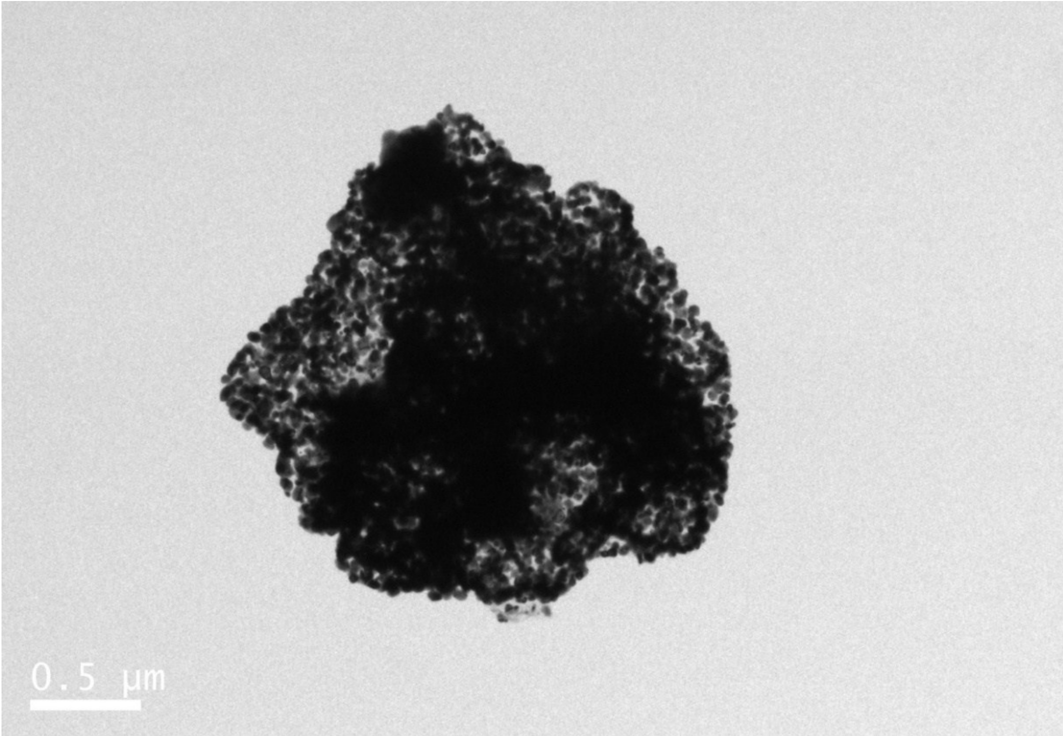

Fig. S2. TEM image of Ni@G.

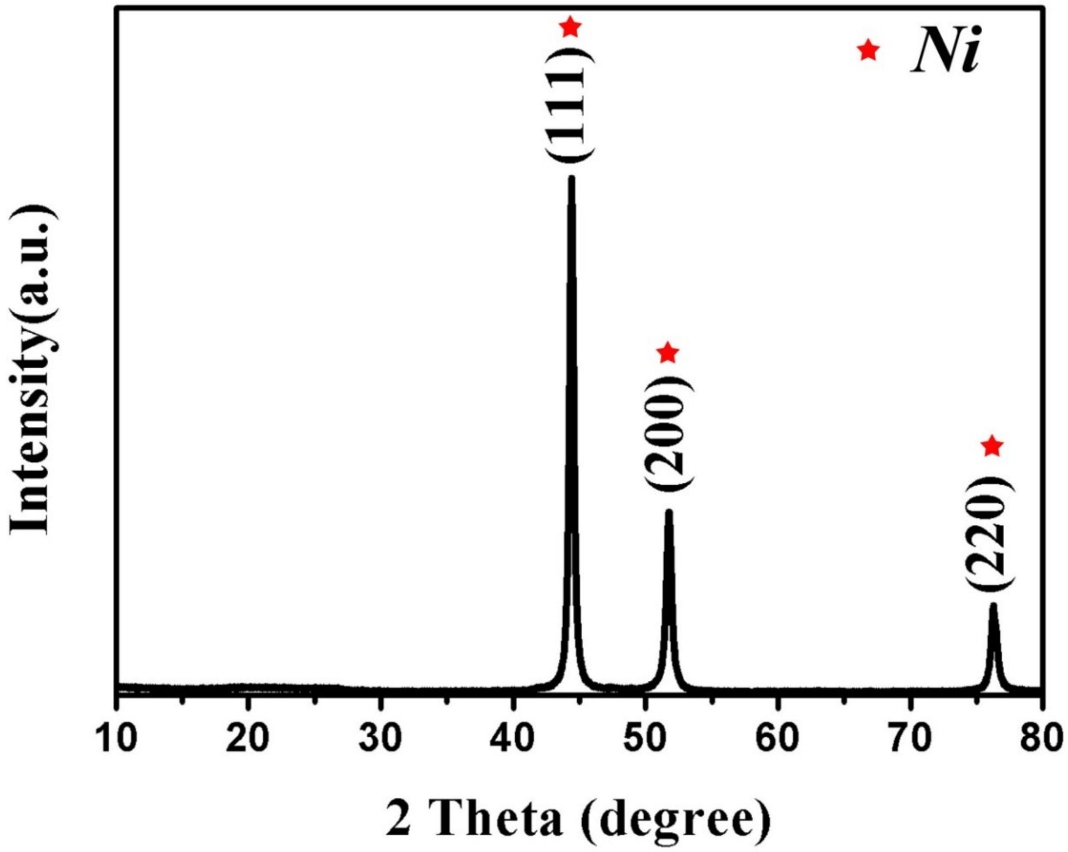

Fig. S3. XRD pattern of Ni@G.

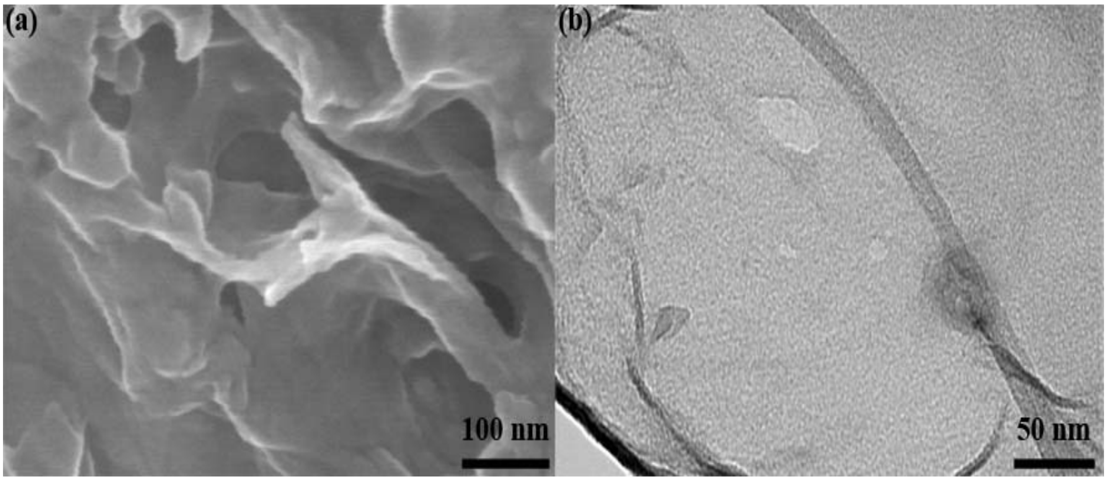

Fig. S4. (a) FESEM and (b) TEM images of porous graphene microspheres.

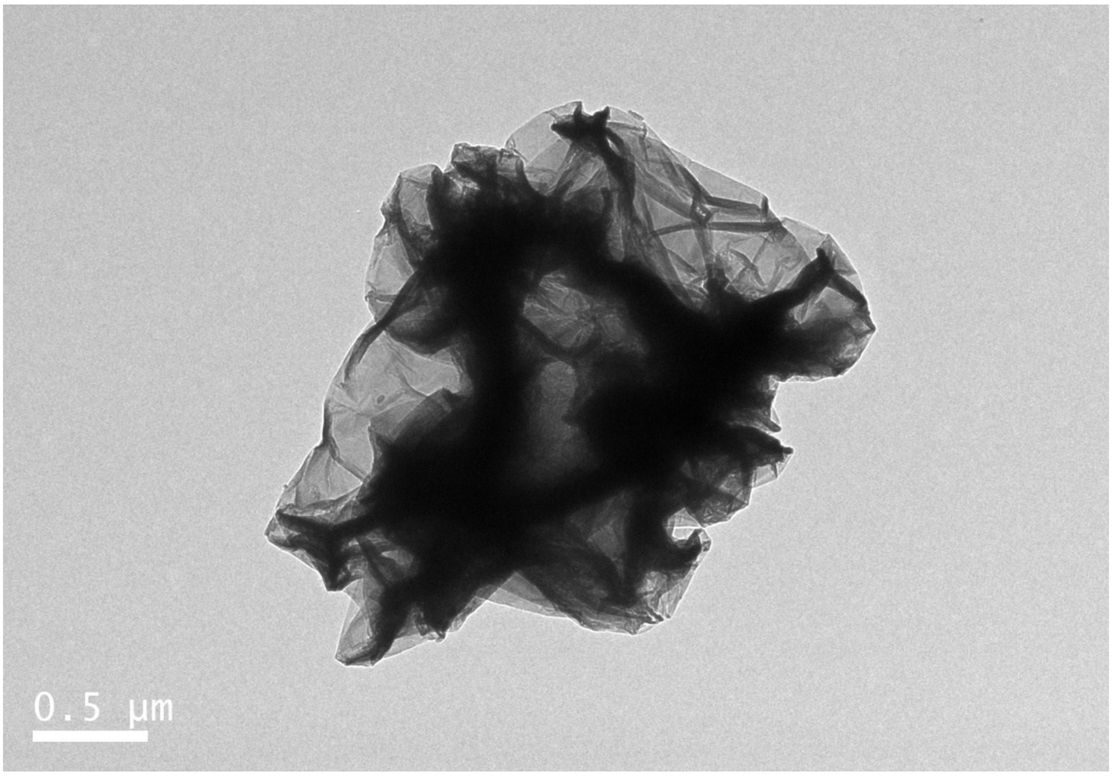

Fig. S5. TEM image of pristine graphene microspheres.

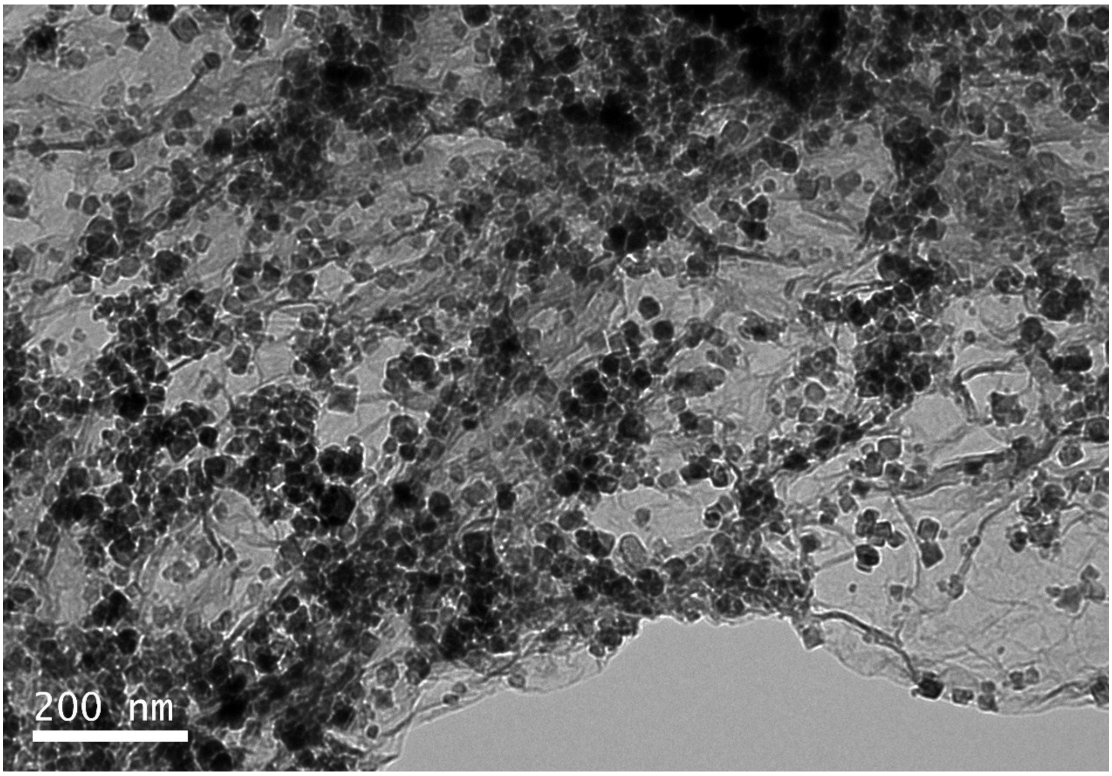

Fig. S6. TEM image of DM-Ni_xS_y@G.

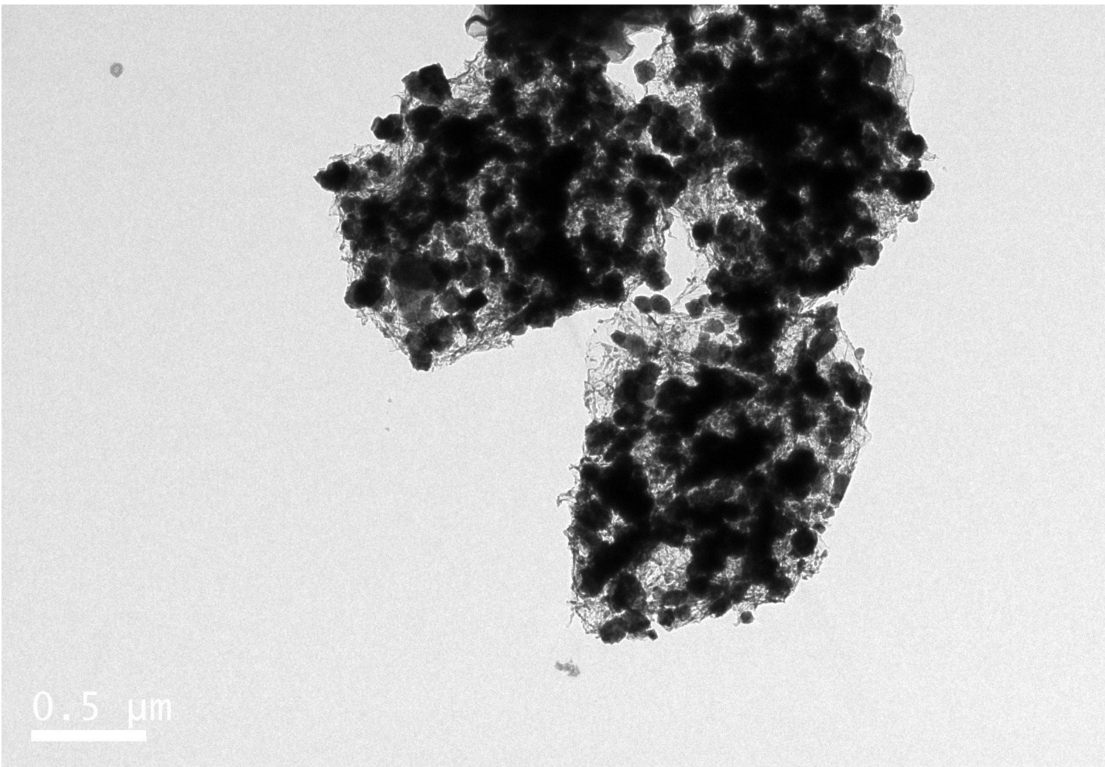

Fig. S7. TEM image of NiS@G.

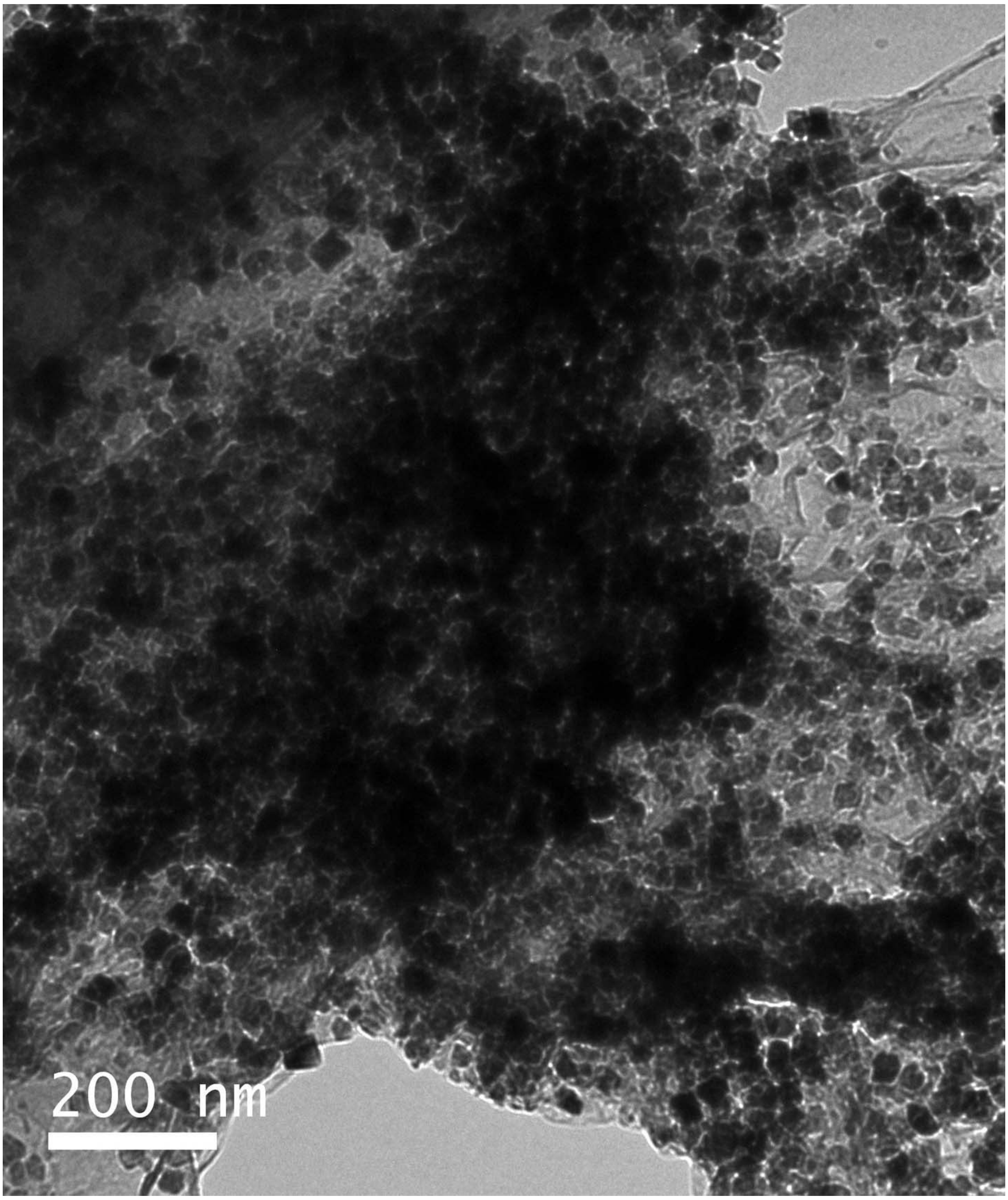

Fig. S8. TEM image of DM-Ni_xS_y@G electrodes after 100000 charge-discharge cycles at 5 A/g.

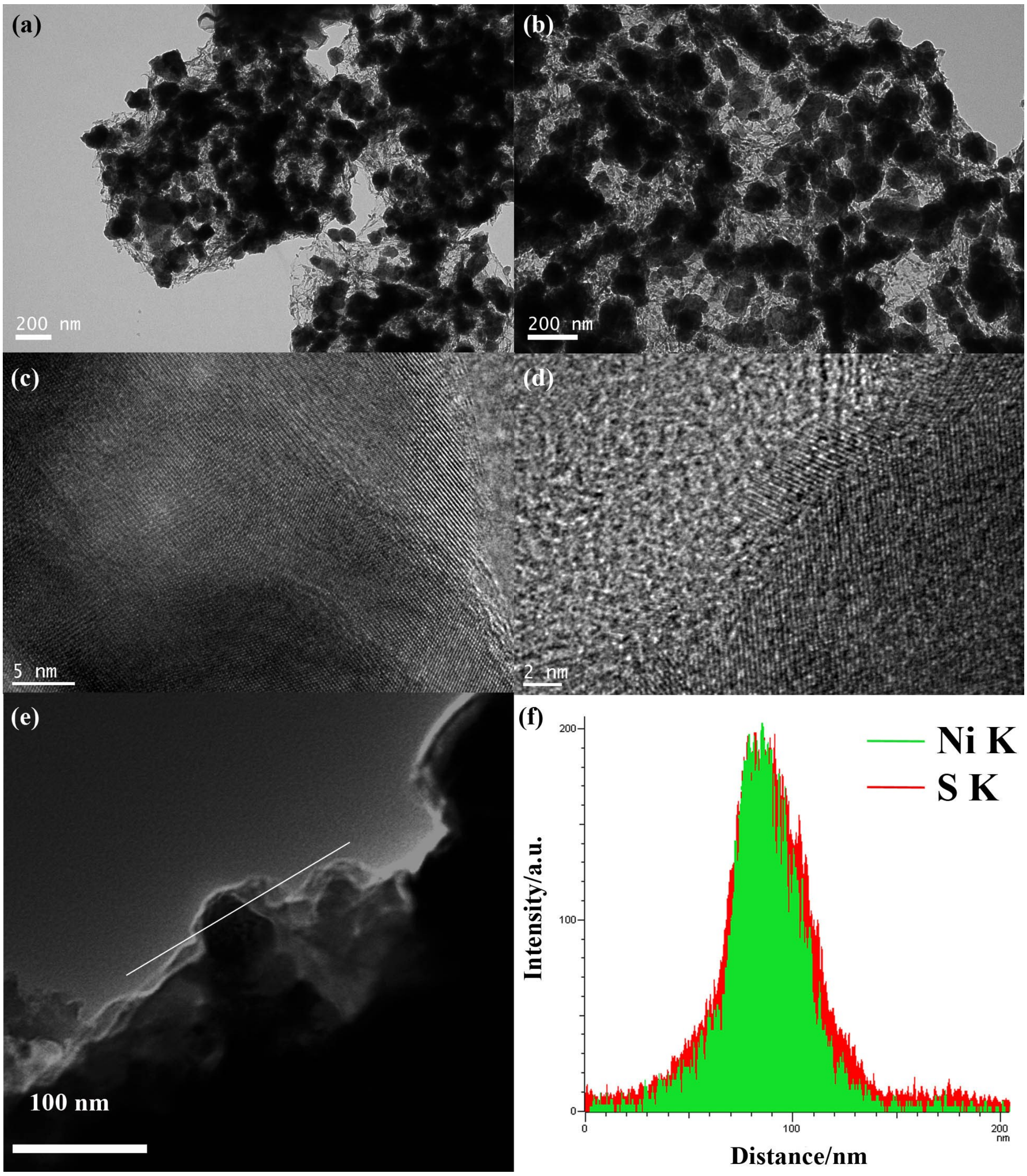

Fig. S9. (a, b) TEM images, (c, d) HRTEM images of PM-Ni_xS_y microflowers. (e) scanning transmission electron microscopy image for STEM/EDS line scan, (f) STEM/EDS line scan profile of binary Ni_xS_y nanobeads in PM-Ni_xS_y microflowers.

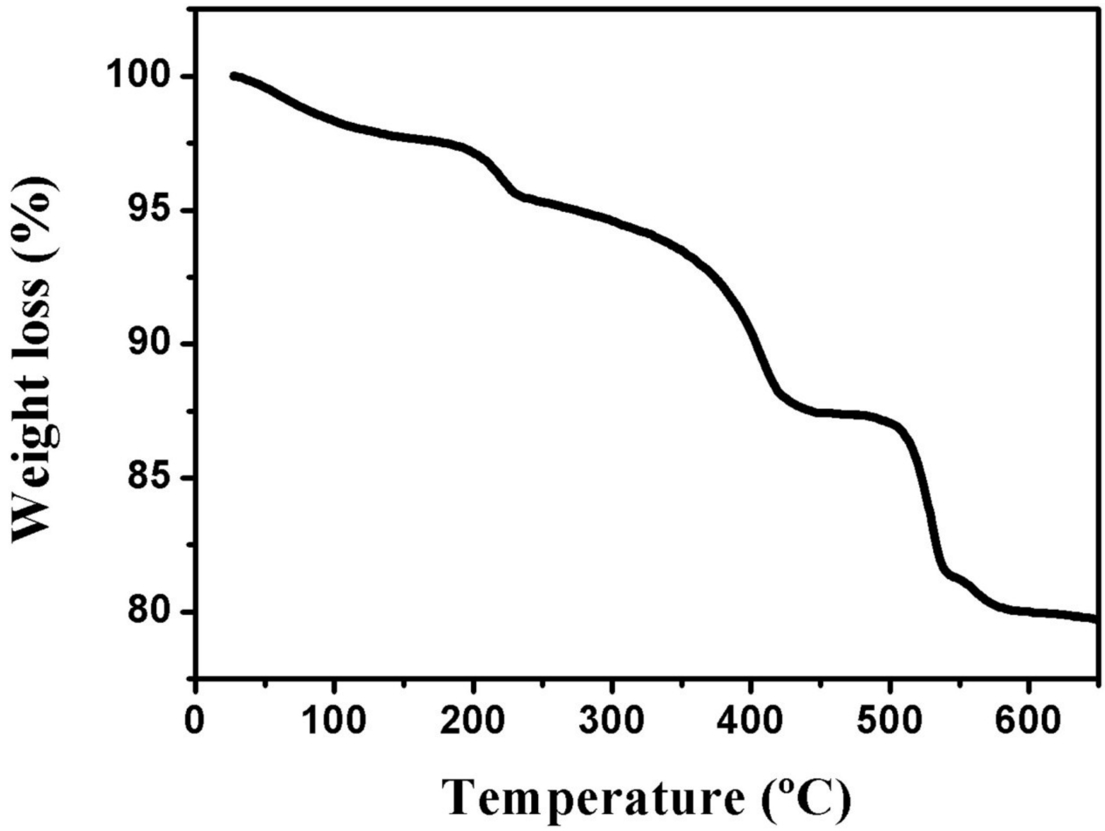

Fig. S10. TGA curve of PM-Ni_xS_y microflowers ranging from 25 to 650 °C at a heating rate of 10 °C /min under air flow.

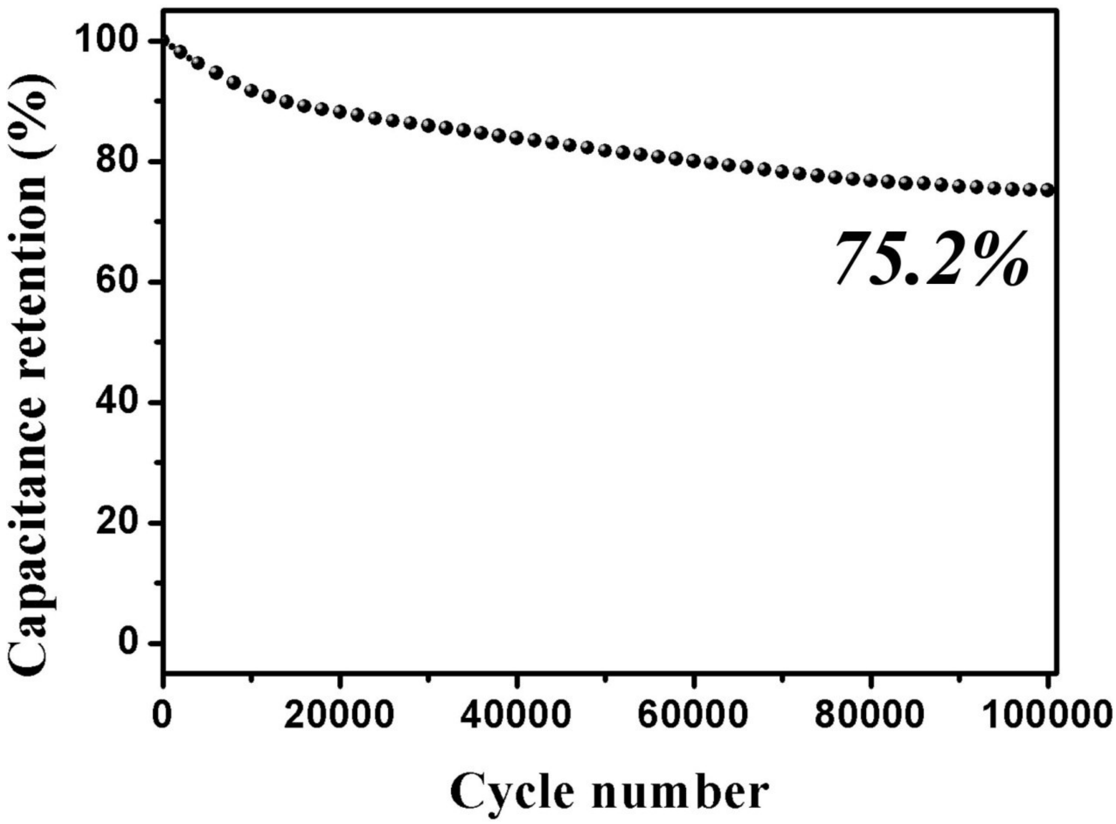

Fig. S11. Cycle performance of the DM-Ni_xS_y@G electrodes.

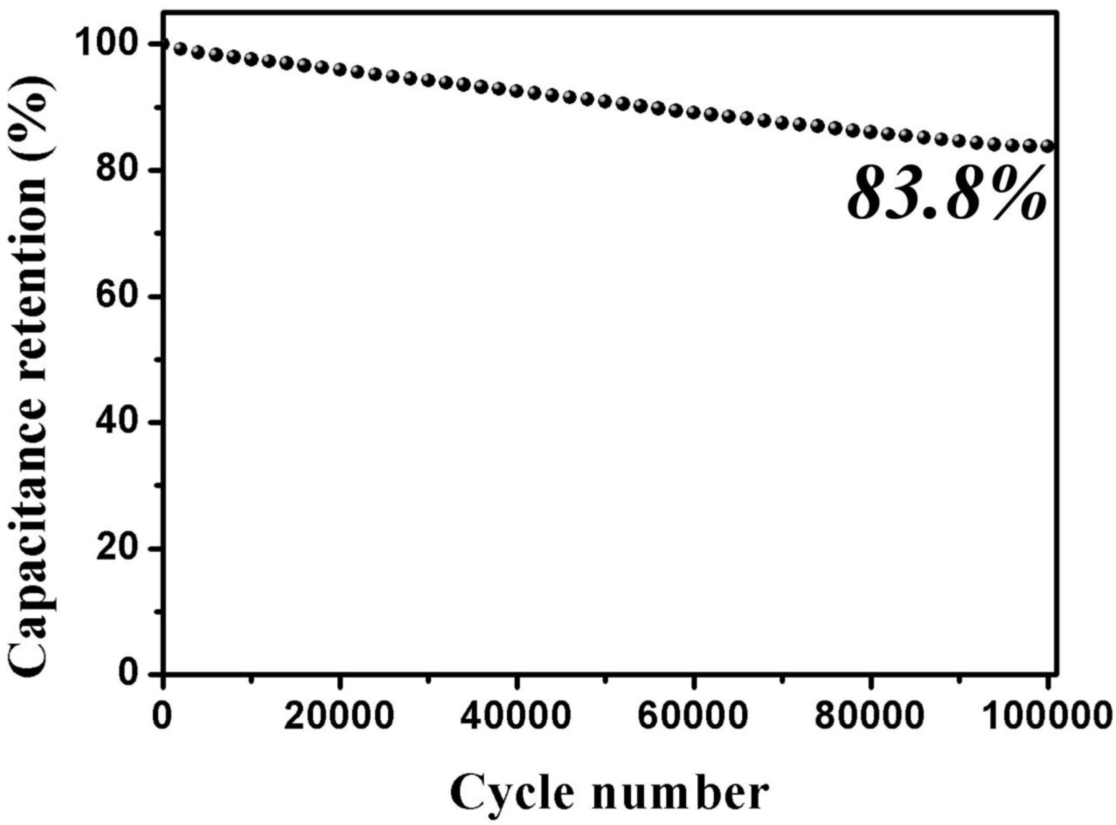

Fig. S12. Cycle performance of the NiS@G electrodes**.**

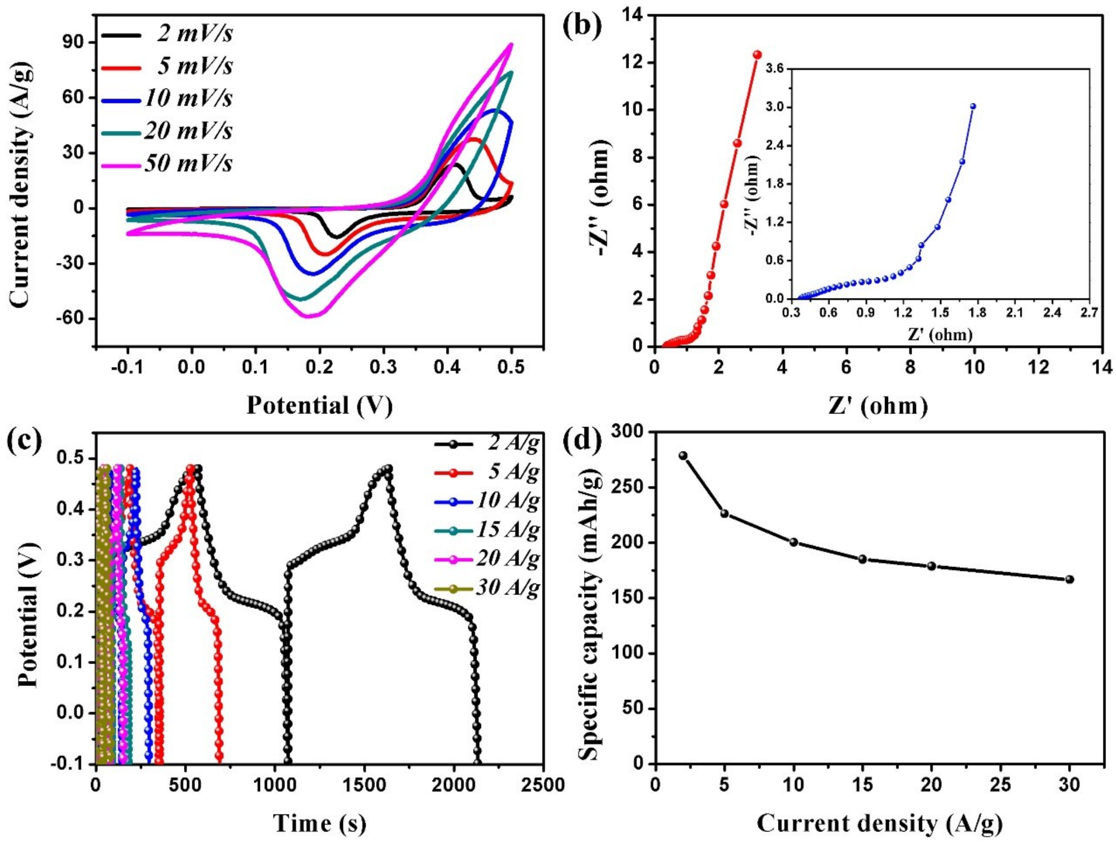

Fig. S13. (a) CV curves at scan rates of 2-50 mV/s; (b) EIS plot; (c) GCD curves; (d) specific capacity at different current densities of 2-30 A/g of DM-Ni_xS_y@G electrodes**.**

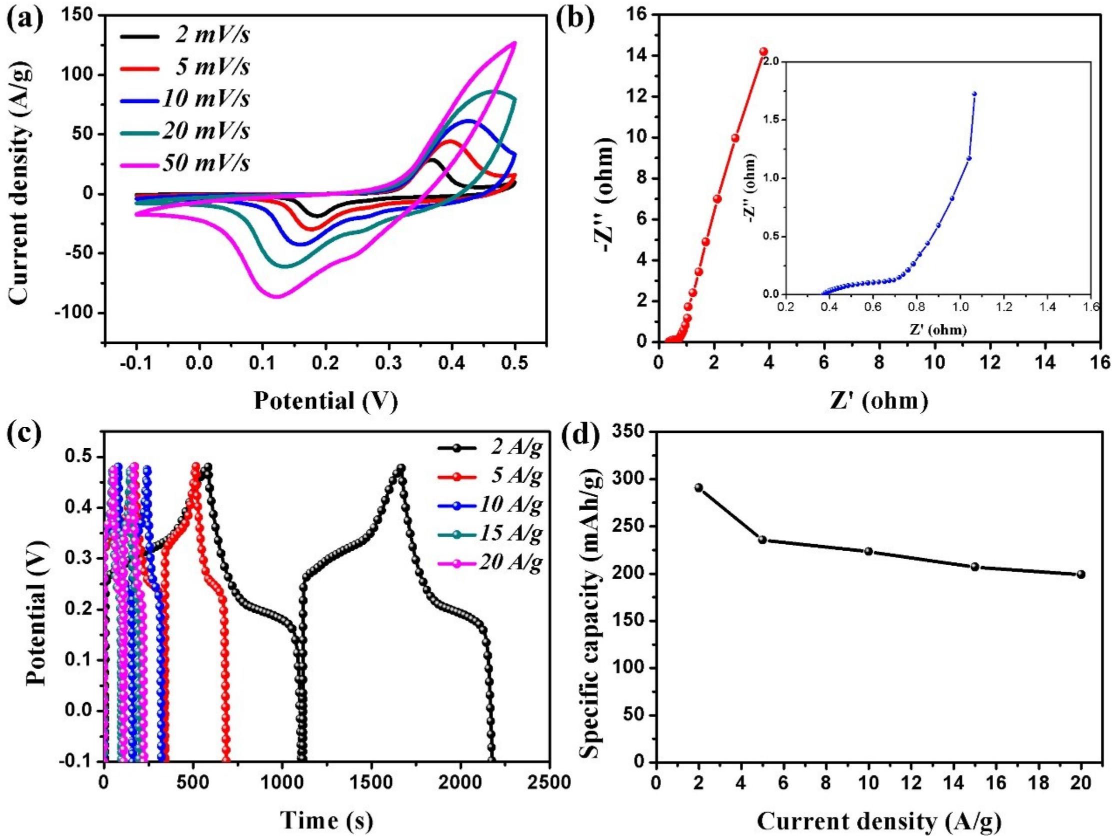

Fig. S14. (a) CV curves at scan rates of 2-50 mV/s; (b) EIS plot; (c) GCD curves; (d) specific capacity at different current densities of 2-20 A/g of NiS@G electrodes**.**

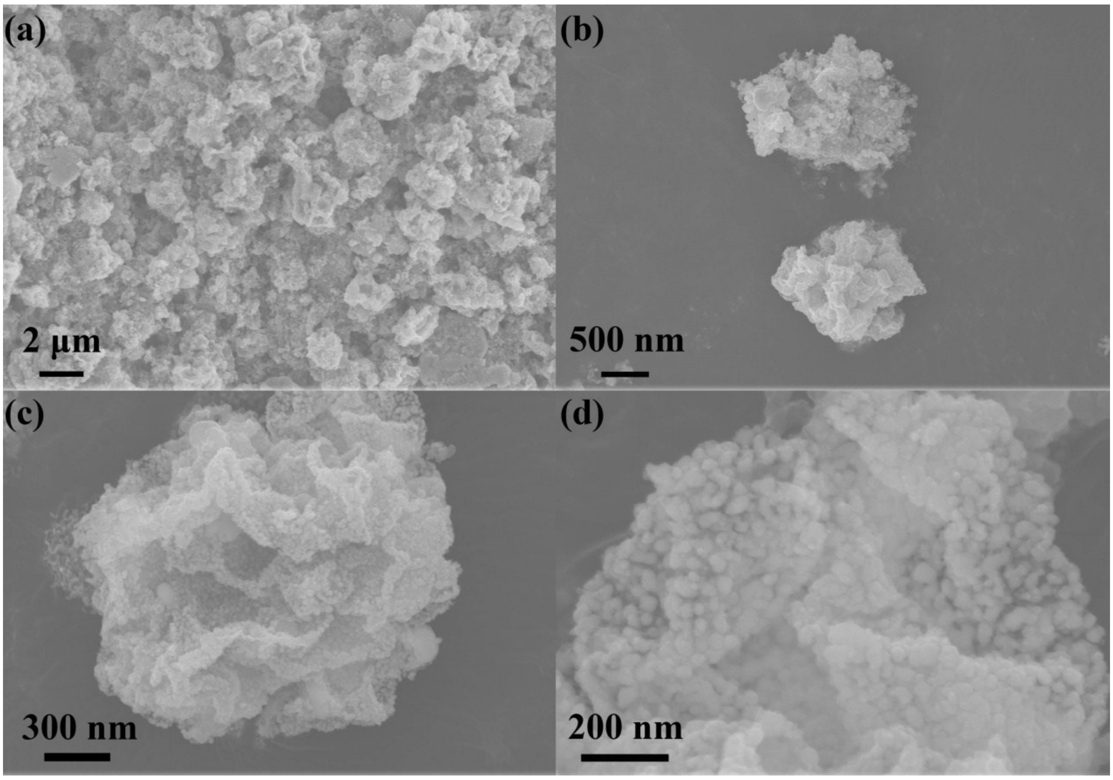

Fig. S15. SEM image of PM-Ni_xS_y electrodes after 100 000 charge-discharge cycles at 5 A/g.

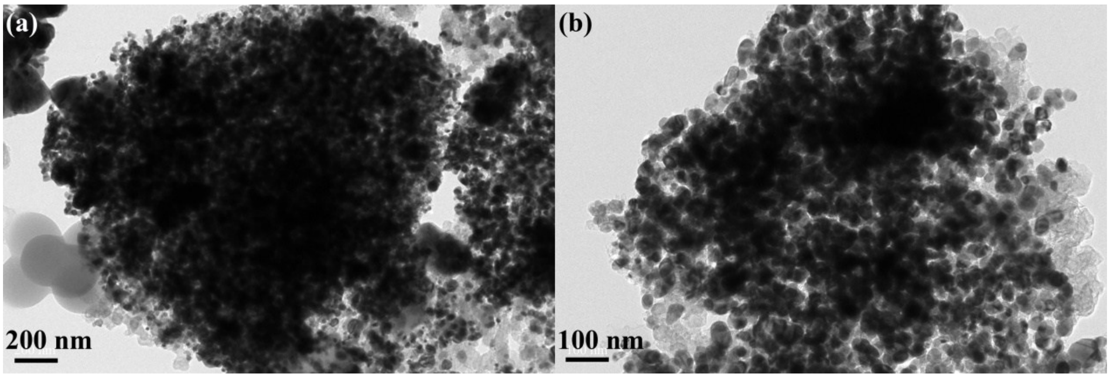

Fig. S16. TEM image of PM-Ni_xS_y electrodes after 100 000 charge-discharge cycles at 5 A/g.

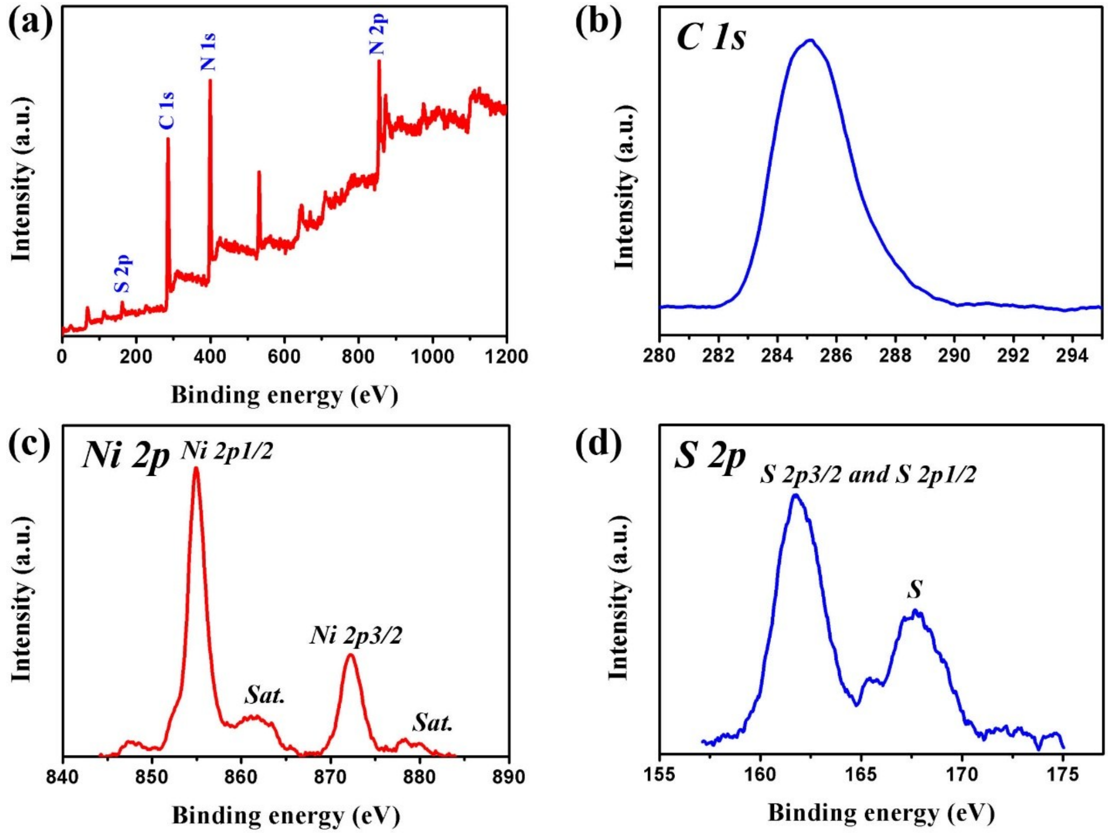

Fig. S17. XPS patterns of PM-Ni_xS_y electrodes after 100 000 charge-discharge cycles at 5 A/g.

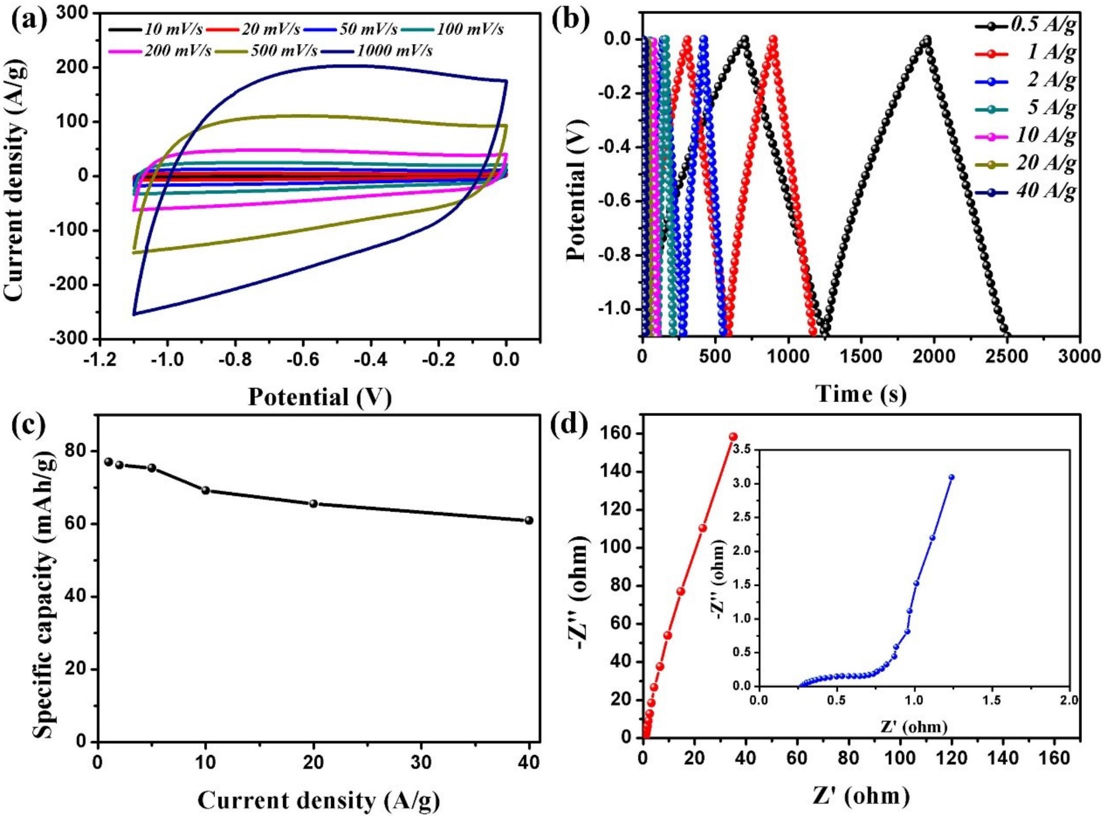

Fig. S18. (a) CV curves at scan rates of 10- 1000 mV/s; (b) GCD curves; (c) specific capacity at different current densities; (d) EIS plot of porous graphene microspheres.

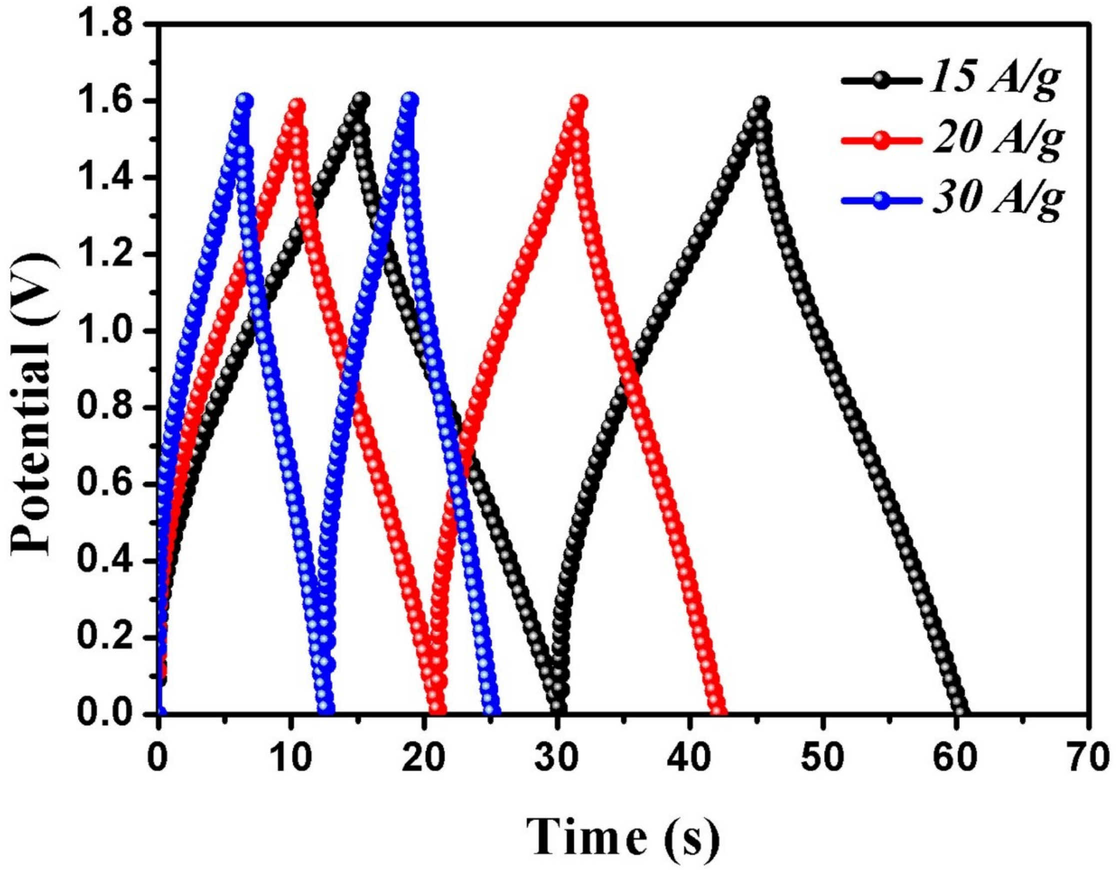

Fig. S19. GCD curves at different current densities of 15-30 A/g of PM-Ni_xS_y//PG ASCs.

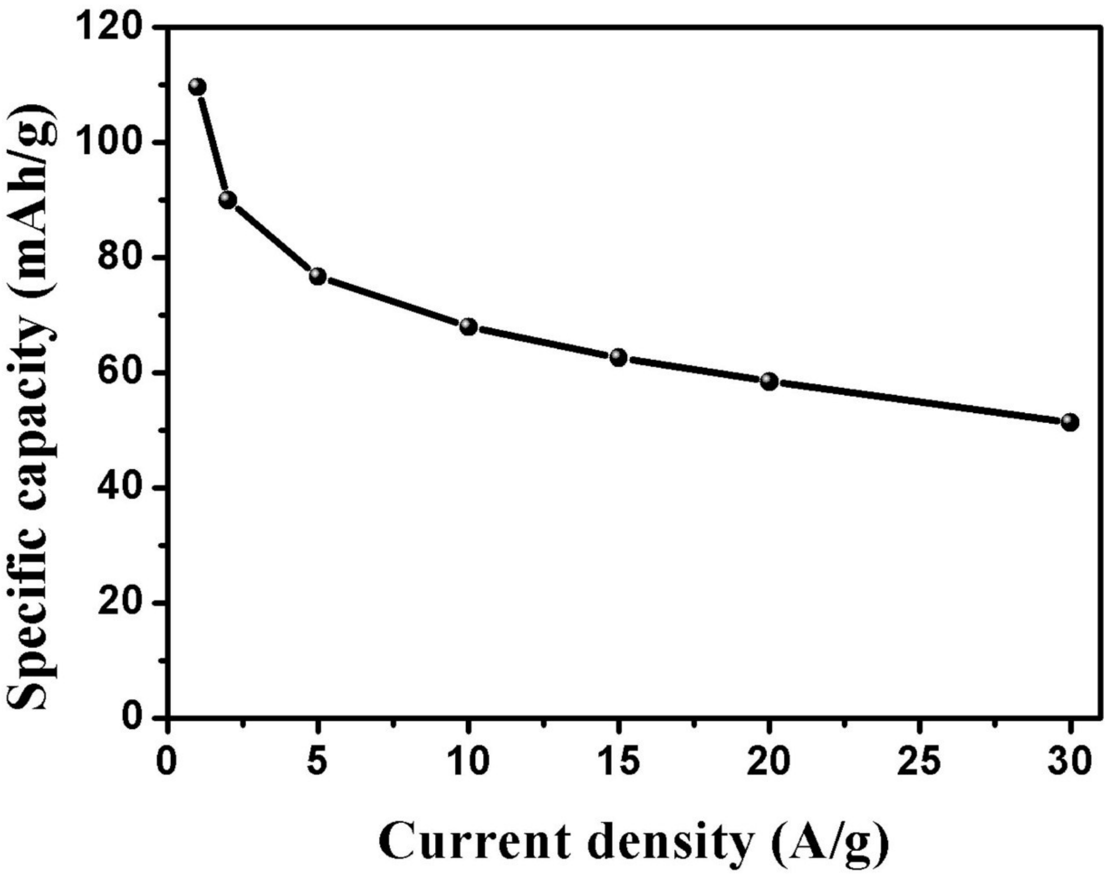

Fig. S20. Specific capacity at different current densities of 1-30 A/g of PM-Ni_xS_y//PG ASCs.

Table S1. Comparision study of the cyclic stability between the PM-Ni_xS_y microflowers electrode in this work and previously reported nickel sulfides based materials.

Materials	Capacitance (F/g)	Cyclic stability	Ref
Ni@rGO-Ni_3S_2	987.8 (1.5 A/g)	97.9% (12 A/g, 3000 cycles)	[1]
Rod-like NiS_2	1020.2 (1 A/g)	93.4% (2 A/g, 2000 cycles)	[2]
NiS microflowers	1122.7 (1 A/g)	97.8% (10 A/g, 1000 cycles)	[3]
Ni_3S_4–MoS_2 heterojunction	985.21 (1 A/g)	85% (10 A/g, 20000 cycles)	[4]
NiS_2/ZnS	1198 (1 A/g)	87% (5 A/g, 1000 cycles)	[5]
NiS/Ni_3S_4 nanosheets	2070.0 (2.5 A/g)	86% (3 A/g, 10000 cycles)	[6]
Ni_3S_2/MWCNT	1024 (0.8 A/g)	80% (3.2 A/g, 1000 cycles)	[7]
Ni_3S_4@MoS_2	1440.9 (2 A/g)	90.7% (10 A/g, 3000 cycles)	[8]
Honeycomb-like NiS_2/NiO	2251 (1 A/g)	78% (5 A/g, 2000 cycles)	[9]
Co-Mo-O/Ni_3S_2/NF	340 (2 A/g)	95.7% (2 A/g, 2000 cycles)	[10]
Co-doped NiS	2141.9 (2 A/g)	75.3% (10 A/g, 3000 cycles)	[11]
$NiCo_2S_4$/carbon sponge	1093 (0.5 A/g)	83% (8A/g, 8000 cycles)	[12]
Ni_xS_y@CoS polyhedrons	2091.4 (2 A/g)	85.2% (5 A/g, 2000 cycles)	[13]
NiS_2/CoS_2	954.3 (1 A/g)	99.9% (5 A/g, 1000 cycles)	[14]
NiS_x@NCV microcapsules	1600 (1 A/g)	94.36% (1 A/g, 5000 cycles)	[15]
PM-Ni_xS_y microflowers	2331.3 (323.8 mAh/g, 2 A/g)	98.9% (5 A/g, 100000 cycles)	This work

Table S2. Comparision study of the cyclic stability, energy density and power density between the PM-Ni_xS_y//PG ASCs in this work and previously reported nickel sulfides based SCs.

Device	Cyclic stability	Energy density (W h/kg)	Power density (kW/kg)	Ref
Ni@rGO-Co_3S_4// Ni@rGO-Ni_3S_2	96.2% after 3000 cycles (12 A/g)	55.16	0.975	[1]
Rod-like NiS_2//rGO	84.1% after 4000 cycles (2 A/g)	32.76	0.954	[2]
NiS-NF//AC	90.6% after 1000 cycles (25 mA/cm^2)	38.4	0.1666	[16]
Ni_3S_4–MoS_2 heterojunction//AC	86.2% after 10000 cycles (10 A/g)	58.43	0.38595	[3]
Co-Mo-O/Ni_3S_2/NF	90.2% after 3000 cycles (12 A/g)	57.9	1.1	[10]
Co-doped NiS//AC	85.1% after 4000 cycles (10 A/g)	54.9	1.5154	[11]
NiS_2-CoS_2//AC	99.1% after 4000 cycles (2 A/g)	29.3	0.7	[14]
Ni_3S_2/MWCNT-NC//AC	90% after 5000 cycles (4 A/g)	19.8	0.798	[7]
Ni_3S_2@β-NiS//AC	97.8% after 10000 cycles (5 A/g)	55.1	0.9259	[17]
NiS_2/ZnS//AC	88.7% after 1500 cycles (5 A/g)	28	0.7489	[5]
Ni_3S_2/CNF//CNF	97% after 2500 cycles (100 mV/s)	25.8	0.425	[18]
R-NiS/rGO//C/NG-A	93.2% after 10000 cycles (20 A/g)	93	0.962	[19]
NiS_x@NCV//NPC	92.4% after 5000 cycles (1 A/g)	48.02	0.8	[15]
PM-Ni_xS_y//PG	97.6% after 100000 cycles (5 A/g)	88	0.81	This work

Table S3. The rated voltage and power of the used equipment in this work.

Equipment	Rated voltage/V	Rated power/W
LED lamp	1.5	3
Electronic motor	2	5
Miniature game machine	1.5	4
Colorful illuminations	3	5
Electronic game machine	3	7

Notes and references

1. D. Ghosh and C. K. Das, *Acs Appl. Mater. Interfaces*, 2015, **7**, 1122-1131.
2. Y. Ruan, J. Jiang, H. Wan, X. Ji, L. Miao, L. Peng, B. Zhang, L. Lv and J. Liu, *J. Power Sources*, 2016, **301**, 122-130.
3. B. Guan, Y. Li, B. Yin, K. Liu, D. Wang, H. Zhang and C. Cheng, *Chem. Eng. J.*, 2017, **308**, 1165-1173.
4. W. Luo, G. Zhang, Y. Cui, Y. Sun, Q. Qin, J. Zhang and W. Zheng, *J. Mater. Chem. A*, 2017, **5**, 11278-11285.
5. G. C. Li, M. Liu, M. K. Wu, P. F. Liu, Z. Zhou, S. R. Zhu, R. Liu and L. Han, *Rsc Adv.*, 2016, **6**, 103517-103522.
6. Y. Li, J. Xu, H. Liu, Y. Liu, M. Wang, J. Li and H. Cui, *J. Sol-Gel Sci. Techn.*, 2018, **87**, 546-553.
7. C. S. Dai, P. Y. Chien, J. Y. Lin, S. W. Chou, W. K. Wu, P. H. Li, K. Y. Wu and T. W. Lin, *Acs Appl. Mater. Interfaces*, 2013, **5**, 12168-12174.
8. Y. Zhang, W. Sun, X. Rui, B. Li, H. T. Tan, G. Guo, S. Madhavi, Y. Zong and Q. Yan, *Small*, 2015, **11**, 3694-3702.
9. D. Zhang, X. Zhou, K. Ye, Y. Li, C. Song, K. Cheng, D. Cao, G. Wang and Q. Li, *Electrochim. Acta*, 2015, **173**, 209-214.
10. K. Tao, Y. Gong, Q. Zhou and J. Lin, *Electrochim. Acta*, 2018, **286**, 65-76.
11. S. Xie, J. Gou, B. Liu and C. Liu, *Inorg. Chem. Front.*, 2018, **5**, 1218-1225.
12. X. Liang, K. Nie, X. Ding, L. Dang, J. Sun, F. Shi, H. Xu, R. Jiang, X. He, Z. Liu and Z. Lei, *Acs Appl. Mater. Interfaces*, 2018, **10**, 10087-10095.
13. R. Gao, Q. Zhang, F. Soyekwo, C. Lin, R. Lv, Y. Qu, M. Chen, A. Zhu and Q. Liu, *Electrochim. Acta*, 2017, **237**, 94-101.
14. H. Zhang, B. Guan, J. Gu, Y. Li, C. Ma, J. Zhao, T. Wang and C. Cheng, *Rsc Adv.*, 2016, **6**, 58916-58924.
15. C. Yang, M. Shi, X. Song, X. Zhao, l. Zhao, J. Liu, P. Zhang and L. Gao, *J. Mater. Chem. A*, 2018, **6**, 5724.
16. L. Yu, B. Yang, Q. Liu, J. Liu, X. Wang, D. Song, J. Wang and X. Jing, *J. Electroanal. Chem.*, 2015, **739**, 156-163.
17. W. Li, S. Wang, L. Xin, M. Wu and X. Lou, *J. Mater. Chem. A*, 2016, **4**, 7700-7709.
18. Y. Wendan, L. Worong, S. Xiaofeng, H. Zhaoxia, L. Ruchun and Y. Dingsheng, *J. Power Sources*, 2014, **272**, 137-143.
19. C. Qu, L. Zhang, W. Meng, Z. Liang, B. Zhu, D. Dang, S. Dai, B. Zhao, H. Tabassum and S. Gao, *J. Mater. Chem. A*, 2018, **6**.